DIFFERENTIAL GMSK RECEIVERS WITH PHASE CONTROL FOR NARROWBAND RADIO COMMUNICATIONS

Ali Mahdavi, Dinah Gordon, Nick Riley
School of Engineering
Hull University
Hull HU6 7RX
England

Abstract

An implementation method for differential Gaussian Minimum Shift Keying receivers with Phase Control is presented. It is shown that in such receivers the effect of InterSymbol Interference (ISI) on the signal, caused by the adjacent bits is reduced by introducing Phase Control in accordance with the data stream. This results in improved system performance, particularly at low values of time-bandwidth product of the premodulation gaussian filter where ISI is high. With the application of this technique the performance of differential receiver is enhanced to a level where it is comparable to that of coherent receiver and yet avoids the problems associated with the complex carrier recovery in the latter case.

Keywords

GMSK Modulation, DSP, Receiver structures.

1. Introduction

In order to facilitate more efficient use of the Radio spectrum the search for optimal digital modulation schemes continues. The ideal technique would require minimum bandwidth for a given data rate, experience minimal degradation over a normal fading and noisy land mobile radio channel, and preferably have a constant envelope to allow the use of class-c non-linear amplifiers.

Gaussian Minimum Shift Keying (GMSK) almost fulfils these requirements. It has a constant envelope with a compact spectrum which currently makes it one of the best options for mobile radio system designs. Beyond its first major application in the GSM system, GMSK is used in several other communication systems such as Digital Cellular System (DCS1800) and wide area data services including RAM Mobile Data (RMD) and Cellular Digital Packet Data (CDPD). Gaussian filtered Frequency Shift Keying (GFSK), which is in fact GMSK with a modulation index of other than 0.5, is adopted by a number of systems such as Digital European Cordless Telephone (DECT) and Cordless Telephone 2 (CT2).

The GMSK signal is generated using either a VCO based or a Quadrature based structure. Although these two structures are equivalent in theory, the quadrature modulator is used in most transmitter systems since it is much easier to maintain the modulation index at exactly 0.5, a prerequisite for coherent demodulation.

GMSK signals can be detected coherently, non-coherently (using limiter discriminator) or differentially, each method possessing advantages and disadvantages in terms of complexity, synchronisation properties and performance. Coherent detection involves complex carrier recovery and has a severe performance degradation if this process is impaired by a typical Rayleigh fading radio channel [1]. Limiter discriminator detection has better synchronisation properties although its Bit Error Rate (BER) performance is poor with respect to that of coherent detection. Differential detection lies between the other two systems in terms of the above factors, and since most radio channels need to operate in a fading environment, this method of detection is often preferred.

In Differential GMSK, the signals can be detected by using an n-bit differential detector (n=1,2,3,...). Previous studies have shown that a 2-bit differential system gives the best performance although still inferior to coherent detection [2].

Whilst implementing various differential systems on a Digital Signal Processor (DSP), the effect on the BER performance of introducing Phase Control (PC) in the delay arm of the detectors is investigated. The PC method is based on first evaluating the ISI contribution of previous bits on the present signal phase and then cancelling its effect, or at least reducing it, by varying the phase delay accordingly.

2. GMSK Modulator

The pulse response of the Gaussian Low Pass Filter (GLPF) of Fig. 1 has a direct influence on the spectrum and performance of the system. This response is determined by the value of the normalised bandwidth B_n which is the product of the 3 dB cut-off frequency of the GLPF, B, and the bit period, T.

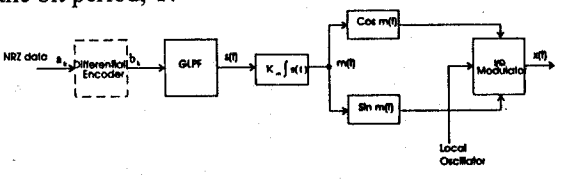

Fig. 1 GMSK Quadrature based modulator

The GLPF can be represented by a FIR filter with a response g(t) to a unit amplitude rectangular pulse of duration T given by

$$g(t) = \frac{1}{2T}\left[Q\left(2\pi B\frac{t-T/2}{\sqrt{\ln 2}}\right) - Q\left(2\pi B\frac{t+T/2}{\sqrt{\ln 2}}\right)\right] \quad (1)$$

for all values of B_n where

$$Q(t) = \int_t^\infty \frac{1}{\sqrt{2\pi}}\exp(-\tau^2/2)d\tau\,. \quad (2)$$

The response g(t) is shown in Fig. 2 for a range of B_n values. g(t) extends over several symbol periods depending on the value of B_n and must be truncated symmetrically over a certain number. A response duration of 4 bits is required for B_n=0.25 and this duration would be increased as B_n is reduced.

The output of the GLPF is expressed as

$$s(t) = \sum_{i=-\infty}^{\infty} b_i g(t-iT) \quad (3)$$

where b is bit polarity. The quadrature based GMSK output is given by

$$x(t) = \cos\omega_c t\cos m(t) - \sin\omega_c t\sin m(t) \quad (4)$$

which is equivalent to the VCO based modulator output

$$x(t) = \cos(\omega_c t + m(t)) \quad (5)$$

where

$$m(t) = k_m\int_{-\infty}^{t} s(\tau)d\tau = k_m\sum_{i=-\infty}^{\infty}(b_i\int_{-\infty}^{t} g(\tau - iT)d\tau)\,. \quad (6)$$

k_m is a constant, chosen in such a way that the contribution of a single phase pulse to the change of the modulated phase m(t) is exactly $\pi/2$.

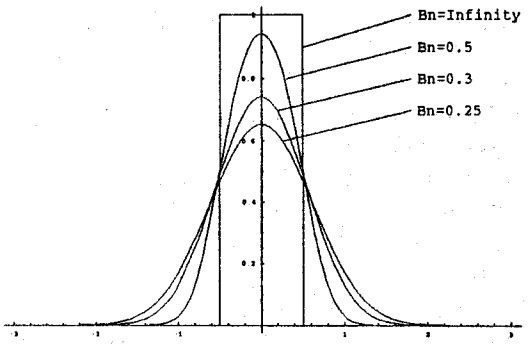

Fig. 2 Response g(t) of GLPF for different B_n values

Fig. 3 demonstrates mathematical models of the instantaneous frequency changes at the output of the GLPF for B_n=0.25, the I and Q-baseband signals and the constant envelope of the GMSK signal.

Referring back to Fig. 1, the differential encoder is required in 2-bit and 3-bit differential systems in order to avoid error propagation in the preceding data bits if a bit error occurs. The data to the encoder is denoted as a_k and the output is denoted as b_k. The differential encoding rule for a 2-bit differential system is given by

$$b_k = -a_k b_{k-1} \quad (7)$$

and for a 3-bit differential system

$$b_k = -a_k b_{k-1} b_{k-2}\,. \quad (8)$$

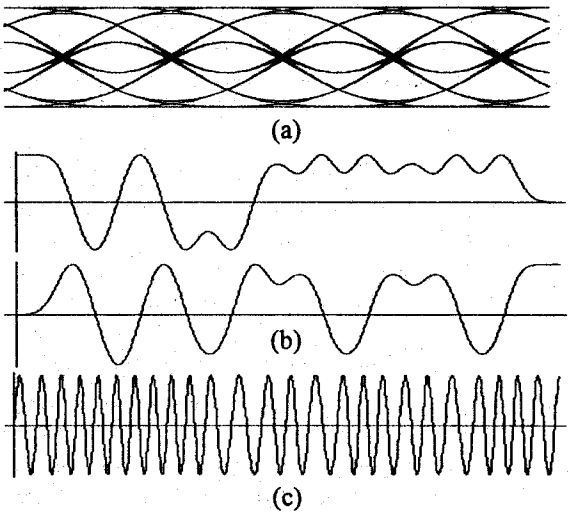

Fig. 3 (a) Eye diagram at the output of GLPF (B_n=0.25)
(b) I and Q-baseband signals
(c) Constant envelope of GMSK signal x(t)

3. Differential Detection

In differential detection of GMSK, a 2-bit differential system provides the best performance. The block diagram of Fig. 4 shows an n-bit differential detector (n=1,2,3,..) with the 90° phase shift only required for odd values of n.

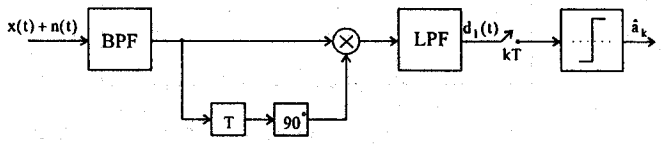

Fig. 4 Block diagram of an n-bit differential detector

In laboratory test, the input to the pre-detection BandPass filter (BPF) is corrupted by Additive White Gaussian Noise (AWGN). The output of the 2-bit differential detector, denoted by d(t), is obtained by LowPass Filtering (LPF) the product of the received signal r(t) and a 2-bit delayed version of itself

$$d(t) = r(t)r(t-2T) = \cos(k_m\sum_{i=-\infty}^{\infty} b_i\int_{t-2T}^{t} g(\tau - iT)d\tau) + n(t)\,. \quad (9)$$

Where $n(t)$ represents all the noise terms. At the time instant kT for k=1,2,3,... , d(t) is given by

$$d(kT) = r(kT)r(kT-2T) = \cos(\sum_{i=-\infty}^{\infty} b_i\theta_{k-i}) + n(kT) \quad (10)$$

where

$$\theta_{k-i} = k_m\int_{kT-2T}^{kT} g(\tau - iT)d\tau\,. \quad (11)$$

The values of θ_i for different B_n values are shown in Table 1 where θ_0 and θ_1 represent the signal phase, and the rest are the ISI terms.

Bn	θ_{-3}	θ_{-2}	θ_{-1}	θ_0	θ_1	θ_2	θ_3	θ_4
0.25	—	0.6	18.8	70.6	70.6	18.8	0.6	—
0.3	—	0.2	16.2	73.6	73.6	16.2	0.2	—
0.5	—	—	10.3	79.7	79.7	10.3	—	—
∞	—	—	—	90.0	90.0	—	—	—

Table 1 Phase shifts in degrees corresponding to the signal and the ISI terms for the 2-bit differential detection

Observe that θ_i is zero for $i \geq 4$ and $i \leq -3$, and that the sum of all the terms in each row is 180° since the modulation index is 0.5. Therefore, equation (10) can now be written as follows

$$d(kT) = r(kT)r(kT-2T) = \cos(\Delta\theta_k) + n(kT) \qquad (12)$$

where $\Delta\theta_k$ is the differential phase angle given by

$$\Delta\theta_k = b_{k+2}\theta_{-2} + b_{k+1}\theta_{-1} + b_k\theta_0 + b_{k-1}\theta_1 + b_{k-2}\theta_2 + b_{k-3}\theta_3. \qquad (13)$$

$\Delta\theta_k$ corresponding to all possible input data combinations for B_n=0.25 is given in degrees in Table 2 and hence the phase state diagram is shown in Fig. 5.

b_{k-2}	b_{k-1}	b_k	b_{k+}	stat	$\Delta\theta_k$ °
+1	+1	+1	+1	a	178.8
-1	-1	-1	-1	a	-178.8
+1	+1	+1	-1	b	141.2
-1	+1	+1	+1	b	141.2
-1	-1	-1	+1	c	-141.2
+1	-1	-1	-1	c	-141.2
-1	+1	+1	-1	d	103.6
+1	-1	-1	+1	e	-103.6
+1	+1	-1	+1	f	37.6
+1	-1	+1	+1	f	37.6
-1	+1	-1	-1	g	-37.6
-1	-1	+1	-1	g	-37.6
+1	+1	-1	-1	h	0.0
+1	-1	+1	-1	h	0.0
-1	+1	-1	+1	h	0.0
-1	-1	+1	+1	h	0.0

Table 2 $\Delta\theta_k$ for all input data combinations in a 2-bit differential system (B_n=0.25).

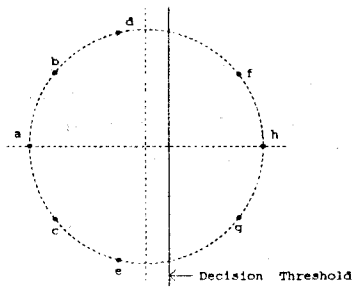

Fig. 5 Phase-state diagram of a 2-bit differential detector (Bn=0.25)

The phase-state diagram highlights the positions of the different phase angles at the sampling instants. It is evident from Fig. 5 that the phase states at the output of the 2-bit differential detector are not symmetrical with respect to the y-axis (decision threshold). The corresponding eye diagram of Fig. 6 for B_n=0.25, obtained on the oscilloscope, confirms this analysis. This asymmetry is only present in 2-bit differential systems and results in performance degradation if the decision threshold is not adjusted accordingly. This is achieved easily on DSP by shifting the decision threshold line to the middle of the misplaced eye.

The minimum differential phase angle $\Delta\theta_{min}$ for a 2-bit detectoris defined as

$$\Delta\theta_{min} = \text{Signal Phase} - 2\sum \text{ISI terms} \qquad (14)$$

and for 1-bit and 3-bit detectors equation (14) is multiplied by a factor of two to take into account the 90° shift. The significance of $\Delta\theta_{min}$ is to determine the lowest B_n value that can be used with each detector, i.e. $\Delta\theta_{min} > 0$. For instance, in a 2-bit detector, $\Delta\theta_{min}$=63.6° for B_n=0.25 and $\Delta\theta_{min}$=20.4° for b_n = 0.18. $\Delta\theta_{min}$ can be calculated for any values of B_n and for any differential detector.

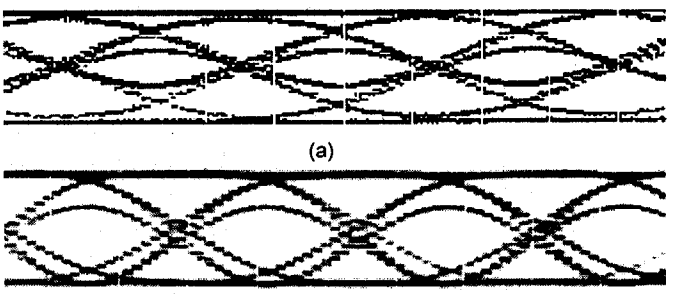

(a)

(b)

Fig. 6 Measured eye diagram for B_n = 0.25 of a conventional 2-bit (a) transmitter, (b) detector

4. Application Of Phase Control

In GMSK, the signal phase is affected by the ISI contributed by the adjacent bits due to the operation of the GLPF in the modulator. Therefore, the information of the previous bits as well as the proceding bits could be present at the decision time instant kT on the present signal phase. There is little that can be done on the effect of the preceding bits that have not yet been received, although the ISI caused by the previous bits can be eliminated, or greatly reduced, as that information is already available prior to the decision time for the present signal. This information is derived by analysing the information presented in the previous section and applying the appropriate phase shift in the delay arm of the differential detector.

Carrying on with the case for the 2-bit detector and B_n=0.25, Fig. 5 shows that the states 'd' and 'e' are the closest states to the decision threshold line y-axis and are subject to maximum amount of ISI. The objective would be to move these states away from this line without bringing any of the other states any closer. Also, by referring to Table 1, it is clear that amongst the ISI terms relating to the previous bits it is only θ_2 that is significantly large for the given values of B_n, therefore, in most cases the effect of the other terms are ignored. With reference to equations (13) and (14) it is now evident that the amount of phase shift,

δ_2, in the delay arm of the 2-bit detector is $2b_{k-2}\theta_2$ given by the following rule

$$\delta_2 = \begin{cases} -2b_{k-2}\theta_2 & \text{if } b_{k-1} \neq b_{k-2} \\ 0 & \text{if } b_{k-1} = b_{k-2} \end{cases} \quad (15)$$

$\Delta\theta_k^{pc}$ is the differential phase angle for a 2-bit detector with PC. Its values corresponding to all possible input data combinations for B_n=0.25 is given in degrees in Table 3 and hence the Phase-state diagram is shown in Fig. 7.

B_{k-}	b_{k-1}	b_k	b_{k+}	stat	$\Delta\theta_k$ °
+1	+1	+1	+1	a'	178.8
-1	-1	-1	-1	a'	-178.8
+1	+1	+1	-1	b'	141.2
-1	+1	+1	+1	b'	178.2
-1	-1	-1	+1	c'	-141.2
+1	-1	-1	-1	c'	-178.2
-1	+1	+1	-1	d'	141.2
+1	-1	-1	+1	e'	- 141.2
+1	+1	-1	+1	f'	37.6
+1	-1	+1	+1	f'	0.0
-1	+1	-1	-1	g'	0.0
-1	-1	+1	-1	g'	-37.6
+1	+1	-1	-1	h'	0.0
+1	-1	+1	-1	h'	37.6
-1	+1	-1	+1	h'	-37.6
-1	-1	+1	+1	h'	0.0

Table 3 $\Delta\theta_k^{pc}$ for all input data combinations in a 2-bit differential system with PC (Bn=0.25).

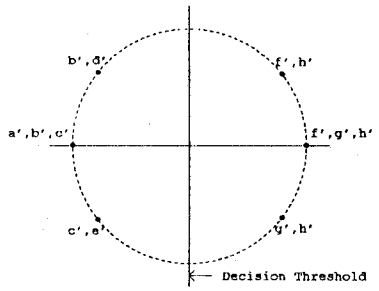

Fig. 7 Phase-state diagram of a 2-bit differential detector with PC (Bn=0.25).

It can be observed from Fig. 7 that all the phase states are now at a further distance from the y-axis as well as being symmetric. In the evaluation of the minimum differential phase angle of equation (14) for the 2-bit detector with PC the ISI terms are now those caused by the future bits only, i.e. θ_i where i<0. $\Delta\theta_{min}$ for B_n=0.25 is now increased from 63.6° to 102.4° indicating a larger eye. A graphical representation from a mathematical modelling and the output of an implementation of this system on DSP are shown in Fig. 8 which both confirm the above analysis.

It is also noted that by using this method lower values of B_n can be achieved for each detector. This would indicate that a smaller transmission bandwidth would be required for a given bit rate whilst maintaining performance.

The structure of a 2-bit differential detector with PC is given in Fig. 9. Note that there is no longer any need to adjust the decision threshold level. Also, the encoder that is required in the modulator of a 2-bit differential system is required in the detector as shown.

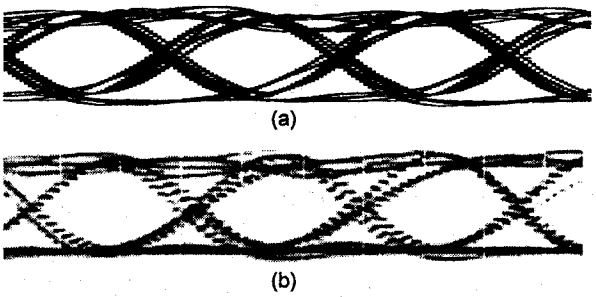

Fig. 8 Eye diagram of the 2-bit detector with PC for B_n=0.25
(a) Mathematical model
(b) Measured on Oscilloscope

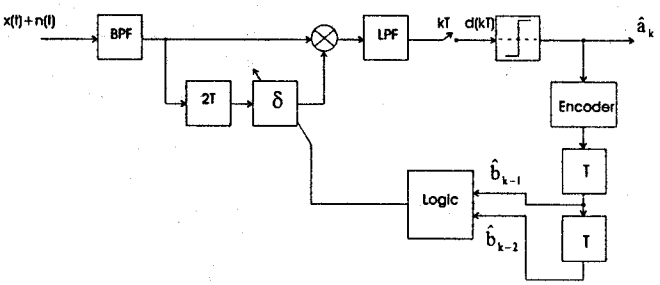

Fig. 9 Block diagram of the 2-bit differential detector with PC

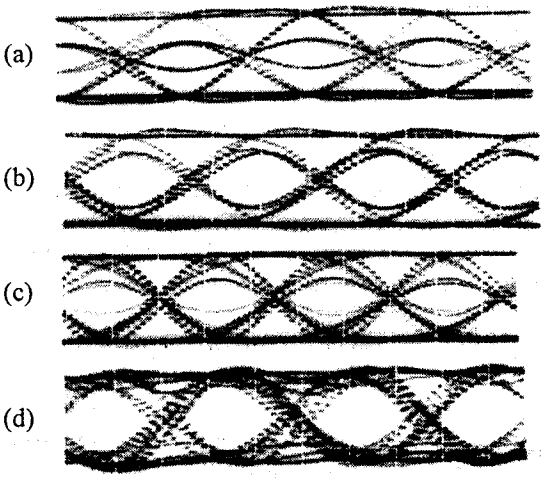

Fig. 10 Measured Eye diagrams of : (a) Conventional 1-bit detector
(b) 1-bit detector with PC
(c) Conventional 3-bit detector
(d) 3-bit detector with PC.

The same mathematical analysis can be applied to other n-bit differential systems [3]. Fig. 10 shows eye diagrams, resulting from DSP implementation tests, for 1-bit and 3-bit detectors with and without the PC for B_n=0.25. It is observed that PC has a significant impact on all of the detectors at low B_n values. This impact becomes less pronounced at higher B_n values where ISI is less.

The amount of phase shift in the delay arm of the 1-bit detector can be formulated as follows

$$\delta_1 = b_{k-1}\theta_1' \quad (16)$$

where θ_1' = 18.2° for B_n=0.25.

Similarly, the amount of phase shift in the delay arm of the 3-bit detector can be formulated as follows

$$\delta_3 = \begin{cases} 2b_{k-3}\theta_3'' & \text{if } b_{k-2} \neq b_{k-3} \\ 0 & \text{if } b_{k-2} = b_{k-3} \end{cases} \quad (17)$$

where $\theta_3'' = 18.8°$ for B_n=0.25.

5. Signal Combining

It has been shown in the last section that in the implementation of differential detectors on DSP application of PC in the delay arm results in an increase in the eye opening in the corresponding eye diagrams. The effect on the performance of designing a receiver based on using the outputs of two of the detectors jointly [3] is now investigated. The first receiver is a combined 1-bit and 2-bit detector both with PC (1+2PC) and the second receiver is a combined 2-bit and 3-bit detectors both with PC (2+3PC).

The structure of the 1+2PC is shown in Fig. 11.

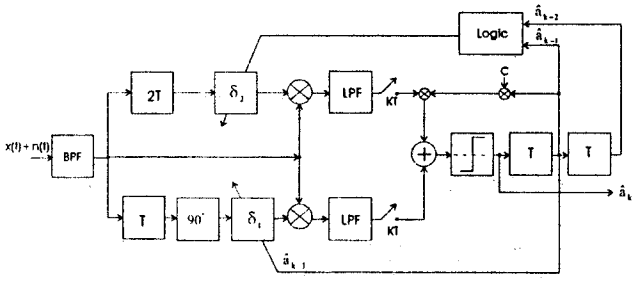

Fig. 11 Block diagram of the 1+2PC receiver

The decision law for this receiver is given by

$$\hat{a}_k = \mathrm{sgn}[d'(kt) - c_1 \hat{a}_{k-1} d(kt)] \quad (18)$$

where d(kt) is the sampled output of the 2-bit detector with PC (2bit-PC), d'(kt) is the sampled output of the 1-bit detector with PC (1bit-PC) and c_1 is the combining coefficient. The transmitter required for this detector does not employ a differential encoder. The eye diagram of this receiver is shown in Fig. 12.

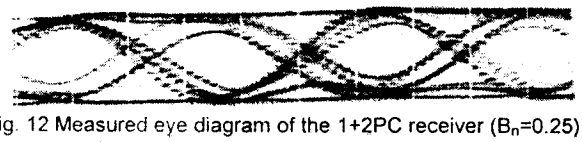

Fig. 12 Measured eye diagram of the 1+2PC receiver (B_n=0.25)

The structure of the 2+3PC is shown in Fig. 13.

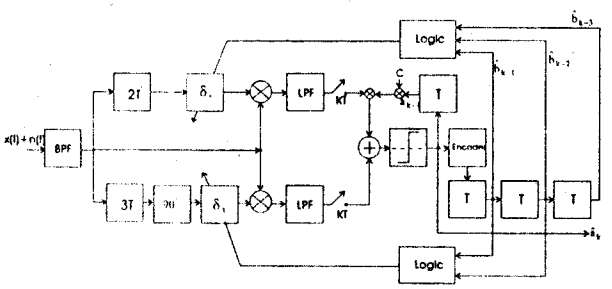

Fig. 13 Block diagram of the 2+3PC receiver

The decision law for this receiver is given by

$$\hat{a}_k = \mathrm{sgn}[d(kt) - c_2 \hat{a}_{k-1} d''(kt)] \quad (19)$$

where d''(kt) is the sampled output of the 3-bit detector with PC (3bit-PC) and c_2 is the combining coefficient. The differential encoder that is required in this system, both in the transmitter and the receiver, is identical to the one used in the 2bit-PC system. The measured eye diagram of this receiver is shown in Fig. 14.

Fig. 14 Measured eye diagram of the 2+3PC receiver (B_n = 0.25)

6. Results

All of the receivers with PC that have been described here require precise phase shifts according to their mathematical analysis. For instance, in a 2bit-PC receiver a phase change of ±37.6° would be required if the previous 2 bits are not identical. The phase shifting process is carried out by manipulating the I and Q channels. The received signal in the receiver DSP is resolved into its I and Q components, using a nominal carrier sinewave, and treated as a complex signal such that

$$V_0 = I + JQ \quad (20)$$

This signal is then multiplied by a complex number of unit amplitude and an appropriate phase.

In the transmitter DSP, the quadrature based modulator of Fig. 1 is implemented and the data bits are generated at 4 kbps with 8 samples/bit and baseband frequency, using a Pseudo Random Binary Sequence (PRBS) generator with a repetition period of $N=(2^{10}-1)$ bits. The GMSK signals are then corrupted with AWGN before transmission through the Digital-to-Analogue Converter (DAC). In the receiver, the received sampled signals at the output of the Analogue-to-Digital Converter (ADC) are filtered in the pre-detection BPF which is performed by a FIR filter. This filter is implemented in DSP with B_rT=1.0 [4], where B_r is the cut-off frequency of the filter. The output of the pre-detection BPF is then demodulated by one of the differential detectors. The regenerated output is then compared with a PRBS generator in the receiver that is in synchronisation with the PRBS generator in the transmitter, for monitoring the bits in error. The decision for each received bit is made by averaging over the central 4 samples and quadrature matched filtering is used for synchronisation purposes, only at the start of transmission followed by a preamble. The results of the BER testing for these receivers are presented in Fig. 15 and Fig. 16 for B_n=0.25.

It is evident that PC improves performance considerably in all of the differential GMSK detectors. The performance of the 1bit-PC is almost identical to that of a conventional 2-bit detector, and the performance of the 2-bit detector is improved by 3 dB at BER=10^{-4} by

applying phase control in its delay arm. It is observed in Fig. 16 that the 1+2PC receiver system clearly provides a better performance than 2-bitPC and can be considered as a better option despite the fact that it requires more processing. The 2+3PC receiver system does not provide a better performance than the 1+2PC receiver which is in contrary to the simulation results of [3]. It is noted that the performances of the receivers with phase control degrade rapidly at low values of E_b/N_0. This is due to bit error propagation as a result of feedback mechanism in the system.

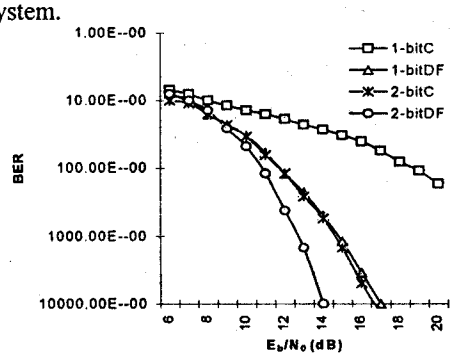

Fig. 15 Performances of the DSP differential GMSK receivers (B_n=0.25)

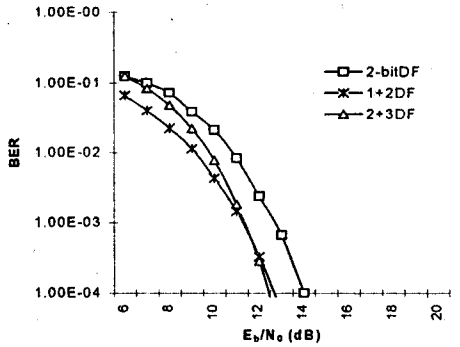

Fig. 16 Performances of the combined output receivers (Bn=0.25)

7. Conclusion

Coherent detection is superior to any of the differential detectors although its poor performance in a Rayleigh fading field has highlighted the need to either optimise its performance by, for instance, adopting diversity techniques where possible, or develop new detection methods. In this paper, an in-depth study of the differential detection of GMSK has been carried out in order to gain an understanding of the effect of the ISI that is introduced by the GLPF of the transmitter on the signal phase. Whilst implementing the differential detectors on DSP it has been shown how the ISI effect may be greatly reduced by applying phase control on the delay arm of the detectors. The BER performance of the combined receivers at B_n=0.25 were in agreement with those of the simulated versions of [3], except for 2+3PC receiver. The 1+2PC differential GMSK receiver is now only about 3 dB (BER=10^{-4}) inferior to coherent detection without the associated problems.

A B_n value of 0.25 has been used for these measurements since it is at this value that maximum spectral efficiency of digital land mobile radio is achieved.

References

[1] S.Goode, "A comparison of Gaussian Minimum Shift Keying to Frequency Shift Keying for Land Mobile Radio", IEEE Vehicular Technology Conference, pp. 136-141, May 1984.

[2] Said M.Elnoubi, "Analysis of GMSK with Two-Bit Differential Detection in Land Mobile Radio Channels", IEEE Trans. on Communications, Vol. COM-35, no. 2, Feb. 1987.

[3] Yongacoglu, D.Makrakis and K.Feher, "Differential Detection of GMSK using Decision Feedback", IEEE Trans. on Communications, Vol. 36. no. 6, June 1988.

[4] M.M.Simon and C.C.Wang, "Differential Detection of Gaussian MSK in a Mobile Radio Environment", IEEE Trans. on Vehicular Technology, Vol. VT-33,no. 4, November 1984.

About authors...

Ali Mahdavi was born in Iran in 1964. He received a B.Eng Honours Degree in Electronic Engineering from The University of Hertfordshire, England, in 1990. After a period of employment with Racal and Ericsson he returned to education by obtaining a Msc in Radio Systems Engineering from The University of Hull, England, in 1994. He is now completing his Ph.D research program in the area of Mobile Communication at Hull.

Dinah Gordon was born in Lincolnshire, England in 1971 and attended Spalding High School for Girls. She received a B.Sc. Honours Degree in Special Mathematics in 1992 and then went on to gain a Ph.D. in Non-Standard Analysis in 1996, both from The University of Hull. She moved to the School of Engineering at Hull, in 1996 where she is now a post-doctoral research assistant working in the area of mobile communications.

Nick Riley was born in Hull, England in 1955 and was educated at Malet Lambert Grammar School, Hull. He received his B.Eng with specialism in Communications Engineering from the University of Sheffield in 1976 and was awarded the Msc in Telecommunications Systems, University of Essex in 1981. After a brief period at the Plessey Allen Clarke Research Centre working on X-band microwave devices, he worked for ten years at the Marconi Research Centre, Great Baddow, Essex (MRC) where he was leader of the Ionospheric Propagation Section, undertaking a wide range of studies in the field of radio systems and radio propagation. He joined the Department of Electronic Engineering at the University of Hull in 1988, where he is now Senior Lecturer in Communication Engineering. Over the past eight years, he has developed research interests in various aspects of radio propagation and radio systems. He is a Chartered Engineer, Member of the Institution of Electrical Engineers and author of over 30 papers on radio and related topics.